

**Molecular Cell, Volume 50**

**Supplemental Information**

**MEK1 Is Required for PTEN Membrane**

**Recruitment, AKT Regulation,**

**and the Maintenance of Peripheral Tolerance**

**Katarina Zmajkovicova, Veronika Jesenberger, Federica Catalanotti, Christian Baumgartner, Gloria Reyes, and  
Manuela Baccarini**

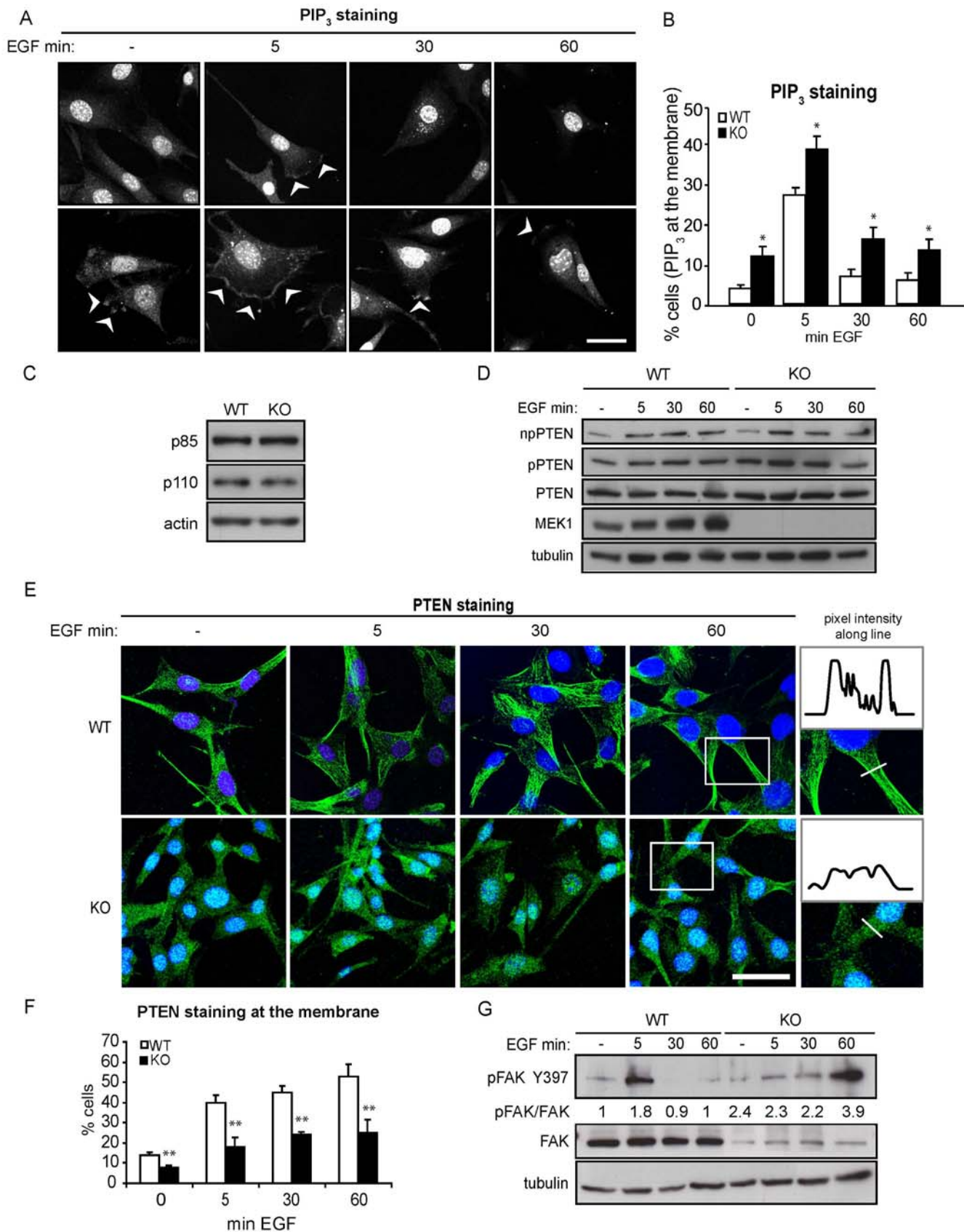


**Figure S1. Impact of MEK1 ablation on PIP<sub>3</sub> signaling, Related to Figure 1**

**A-B**, Increased accumulation of PIP<sub>3</sub> at the membrane of KO cells upon EGF stimulation. WT and KO MEFs were stimulated with EGF for the indicated times. After fixation, cells were stained with a PIP<sub>3</sub> antibody. The arrows indicate accumulation of PIP<sub>3</sub> at the leading edge of the cells. Quantification of PIP<sub>3</sub> staining is shown in (B). **A**

minimum of 100 cells per slide were counted. The graph shows the mean of three experiments  $\pm$  SD. \* < 0.05; \*\* < 0.01; \*\*\* < 0.001. Scale bar 30  $\mu$ m. **C**, Expression of PI3K subunits is equal in WT and KO MEFs. Whole cell lysates from WT and KO MEFs were immunoblotted with the indicated antibodies. Actin is shown as a loading control. **D**, PTEN expression and phosphorylation is not altered in KO MEFs. To assess PTEN expression and phosphorylation (residues S380, T382 and T383; pPTEN = phosphorylated PTEN; npPTEN = non-phosphorylated), WT and KO whole cell lysates prepared at different times after EGF stimulation and the indicated antigens were detected by immunoblotting. Tubulin is shown as a loading control. **E-F**, inefficient PTEN membrane recruitment in EGF-stimulated KO MEFs. Cells were fixed at the indicated time points and stained with a PTEN antibody (green). Nuclei were visualized by DAPI (blue). Scale bar=30  $\mu$ m. Left panels show the PTEN staining intensity along the indicated lines. **F**, Quantification of cells with membrane localization of PTEN was performed by counting at least 300 cells per experimental condition. The plot represents the mean of three independent experiments  $\pm$  SD. \* < 0.05; \*\* < 0.01; \*\*\* < 0.001. **G**, Phosphorylation of FAK Y397 is increased in KO MEFs. WT and KO whole cell lysates prepared at different times after EGF stimulation and the indicated antigens were detected by immunoblotting. Tubulin is shown as a loading control. The quantification was performed in ImageJ. pFAK values were divided by total FAK values. Numbers represent values relative to the unstimulated WT sample, arbitrarily set to 1. In the KO, FAK phosphorylation increases at 60 min after EGF stimulation, even if some PTEN reaches the membrane at this stage. However, the amount of PTEN localized to the KO membrane is low (20% of the WT at the 45 min time point) and doesn't even reach the amount of membrane PTEN observed in the unstimulated WT cells. This would allow the accumulation of the phosphorylated form of FAK. It is also possible that the KO impairs the recruitment of PTEN to membrane domains, such as adherens junctions, in which FAK is enriched, resulting in a disproportionate increase of FAK phosphorylation.

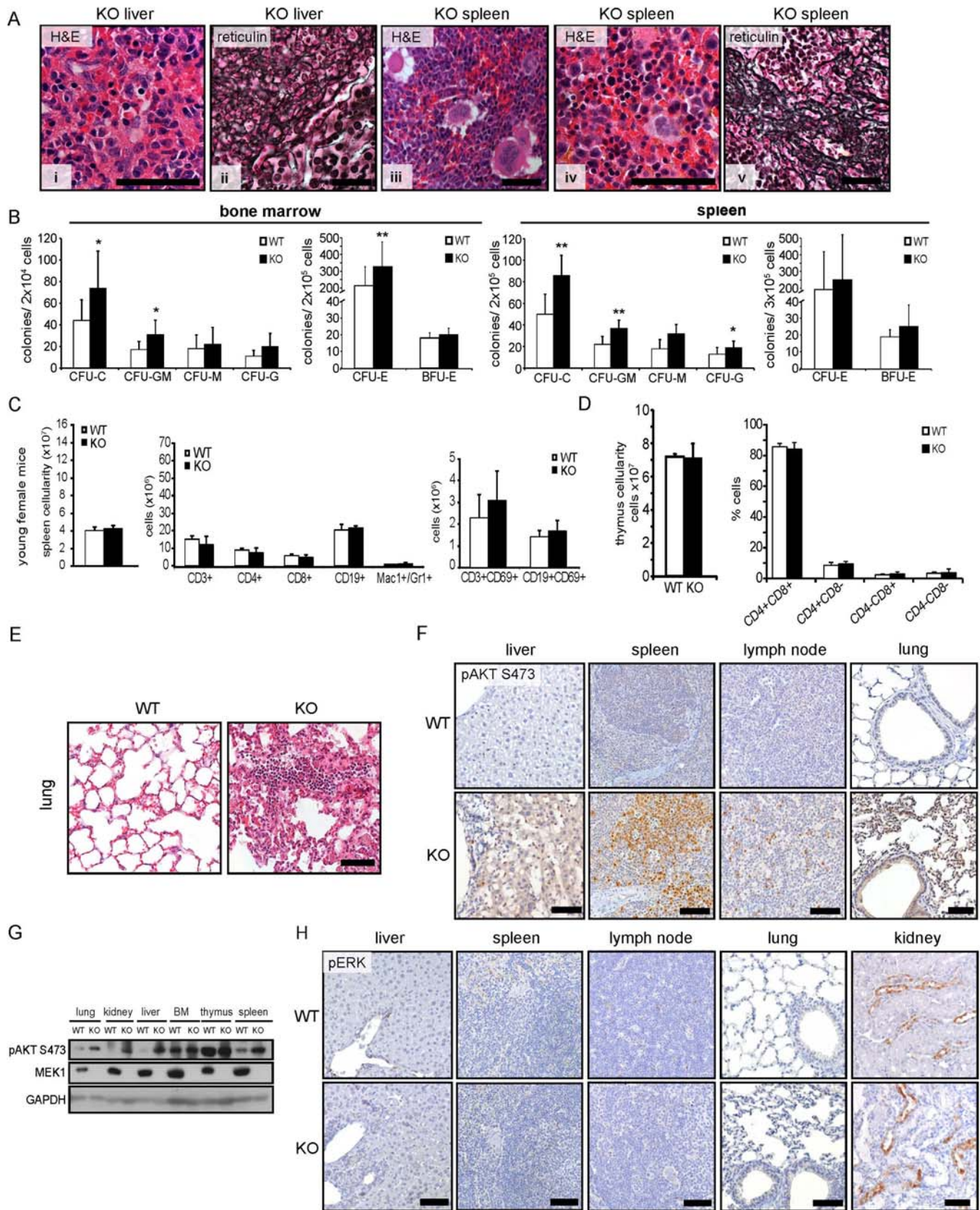


**Figure S2. Phenotypes of MEK1 KO mice, Related to Figure 2**

**A**, Extramedullary hematopoiesis in KO liver (panel i, H&E) and spleen (iv, H&E), accumulation of atypical megakaryocytes in KO spleen (iii, H&E), and fibrosis in liver (ii, reticulin stain) and spleen (v, reticulin stain) are

shown at higher magnification. Scale bar 30 $\mu$ m. **B**, Colony forming units from bone marrow and spleen were determined in young mice (5-8 weeks, n=5). CFU-C= total myeloid colonies, CFU-GM= granulocyte/monocyte colony forming units, CFU-G= granulocyte colony forming units, CFU-M= monocyte colony forming units, BFU-E= burst forming units, CFU-E= colony forming units erythroid. Values represent mean  $\pm$  SD. **C**, Normal spleen cellularity and splenocyte subsets in young female mice (age 1-3 months, n=5), detected by FACS analysis of lineage-specific and activation-induced markers (CD69). Values represent mean  $\pm$  SD of 5 mice. **D**, Normal thymic development in MEK1-deficient mice. Cellularity and composition of thymi isolated from 8 week-old WT and KO females (n =6). Thymocytes were stained for the indicated lineage-specific surface markers and analyzed by FACS. Values represent mean  $\pm$  SD. **E**, Thickening of interstitial alveolar spaces and vascular congestion in H&E stained lung section from a representative 1 year old couple. Scale bar 200 $\mu$ m. **F-G**, AKT phosphorylation in MEK1 KO organs. **F**, Livers, spleens, lymph nodes, and lungs, were dissected, sectioned and stained with an antibody against pAKT S473 (n=3). Representative sections from a 1 year old couple are shown. Scale bar 100 $\mu$ m. **G**, Western blot analysis of organ lysates isolated from a representative 11 month-old mouse and a sex-matched littermate. **H**, Livers, spleens, lymph nodes, lungs and kidneys were dissected, sectioned and stained with an antibody against pERK (n=3). Representative sections from a 1 year old couple are shown. Scale bar 100 $\mu$ m.

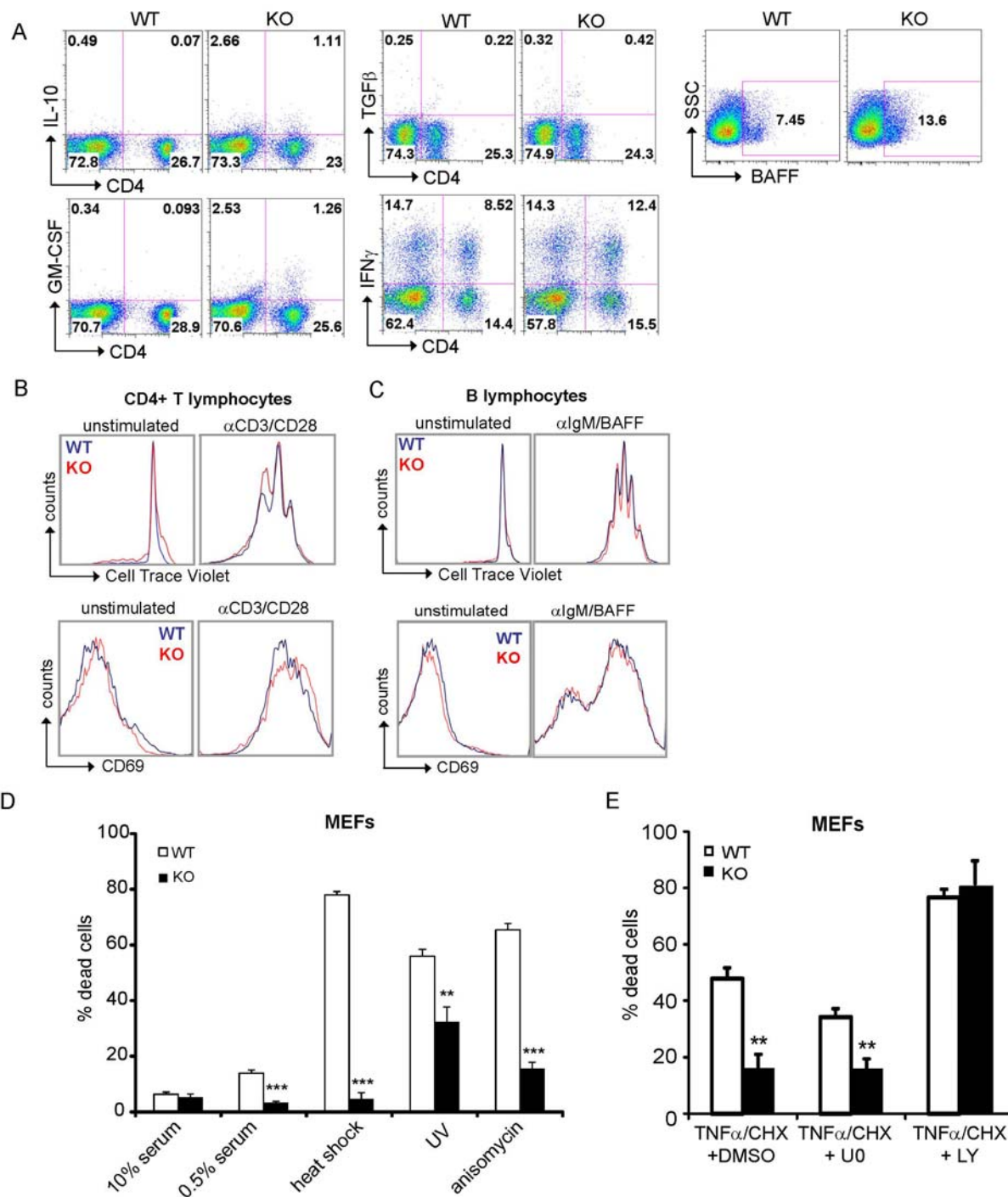


**Figure S3. MEK1 ablation leads to systemic autoimmune disease, Related to Figure 3**

**A**, Cytokine profiles of splenocytes from 8-10 months old mice. Total splenocytes were stimulated in vitro. Cells positive for CD4 and the indicated cytokines were detected by FACS. The plots show one representative littermate pair out of three. **B-C**, Proliferation (upper panels) and expression of the activation marker CD69 (lower panels) was monitored in CD4+ T cells and B cells activated in vitro. Histograms show the results of one representative experiment out of three independent experiments. **D-E**, WT and KO MEFs were grown in medium containing 10% FCS or exposed to different apoptotic stimuli: starvation in 0.5% FCS, heat shock for 30 min at 42°C, UV irradiation 780 J/m<sup>2</sup>, anisomycin (10μg/ml), or TNFα (10ng/ml)/cycloheximide (5μg/ml) for 16 hours. Values represent means ± SD from triplicate samples. One representative experiment is shown. In **E**, WT and KO MEFs were pretreated for 1 hour with UO126 (10 μM), LY294002 (50 μM) or DMSO (vehicle). Cell death was measured by FACS (PI). Results are normalized to spontaneous cell death, values represent mean ± SD. \* < 0.05; \*\* < 0.01; \*\*\* < 0.001.

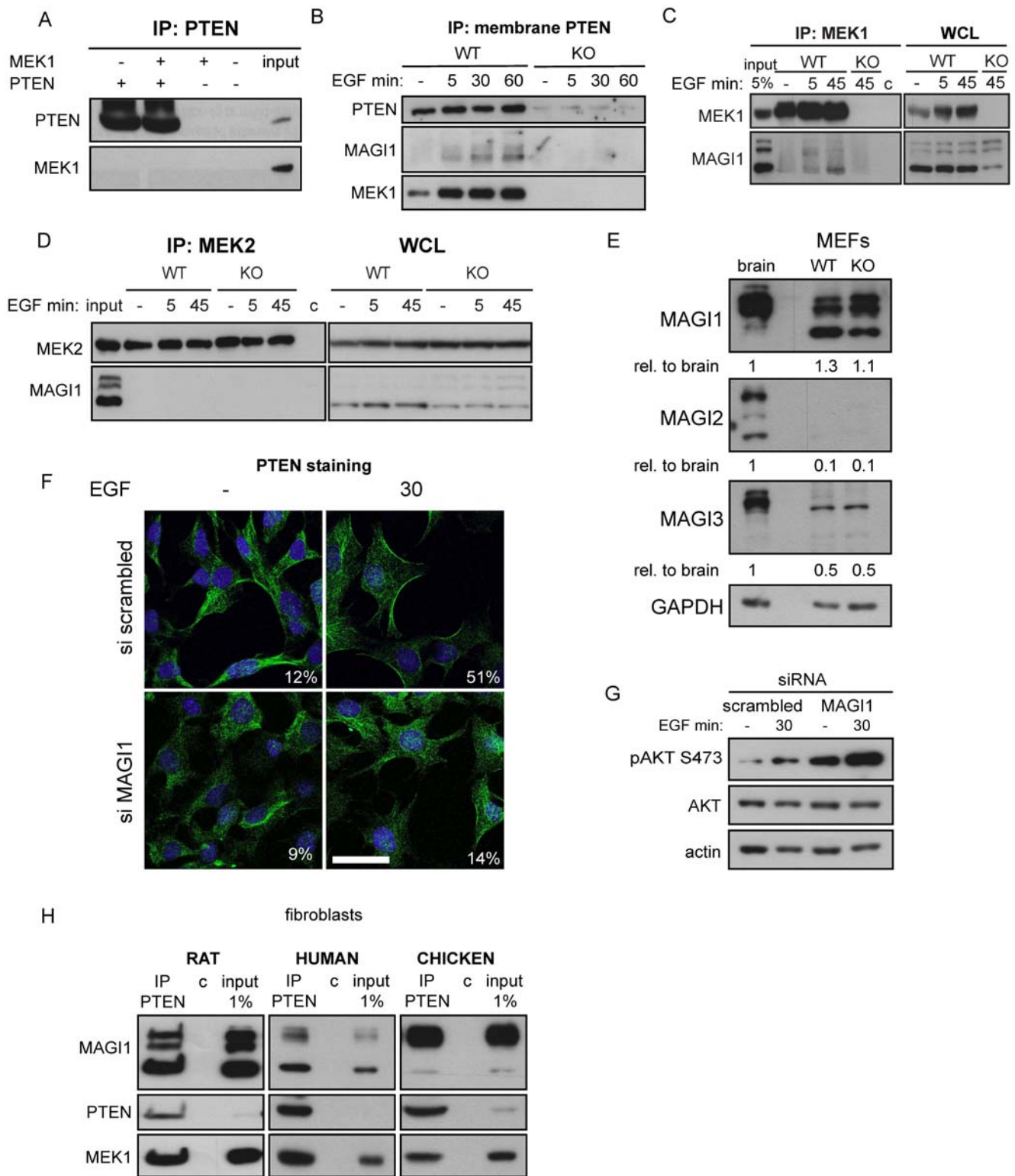


**Figure S4. MEK1 interacts with PTEN via MAGI, and MAGI plays a role in PTEN membrane recruitment and AKT phosphorylation, Related to Figure 4**

**A**, MEK1 does not interact with PTEN directly. Recombinant purified MEK1 (1 $\mu$ g) and PTEN (1  $\mu$ g) were co-incubated prior to PTEN immunoprecipitation and immunoblotting with the indicated antibodies. **B**, EGF stimulation increases the amount of MAGI1<sub>100</sub> and MEK1 co-immunoprecipitated with membrane PTEN. PTEN was immunoprecipitated from the membrane fraction of EGF-stimulated MEFs. PTEN, MEK1 and MAGI1 were detected

by immunoblotting. **C-D**, MEK1, but not MEK2, binds to MAGI1. MEK1 (C) or MEK2 (D) were immunoprecipitated from EGF-stimulated WT and KO MEFs. MAGI1 coimmunoprecipitation was examined by immunoblotting. **c**, unspecific binding to beads. **E**, MAGI1 is the main MAGI protein expressed in WT and KO MEFs. Immunoblot comparing the amounts of MAGI1, MAGI2, and MAGI3 expressed in MEFs and with those present in brain lysates, which contain all three and are therefore used as a reference. The numbers represent the ratio between the amount of MAGI proteins contained in the MEF and brain lysates, normalized for GAPDH content (loading control; all determined by densitometry). All three MAGI1 isoforms were taken into account in this calculation. **F-G**, Knockdown of MAGI1 impairs PTEN membrane translocation and induces AKT activation. WT MEFs transfected with siRNA against MAGI-1 or control siRNA (scrambled) were starved, stimulated with EGF for 30 min and stained for PTEN (green) and DNA (DAPI, blue) (F; Scale bar 30  $\mu$ m). The percentage of cells showing PTEN membrane localization is shown in the insets. In G, whole cell lysates were immunoblotted with phosphospecific AKT antibodies and AKT antibodies to determine the degree of AKT phosphorylation. Actin is shown as a loading control. **H**, Primary fibroblasts from rat, human and chicken continuously growing in the presence of 10% serum were lysed and subjected to PTEN IP. **c**, control for unspecific binding to the beads.



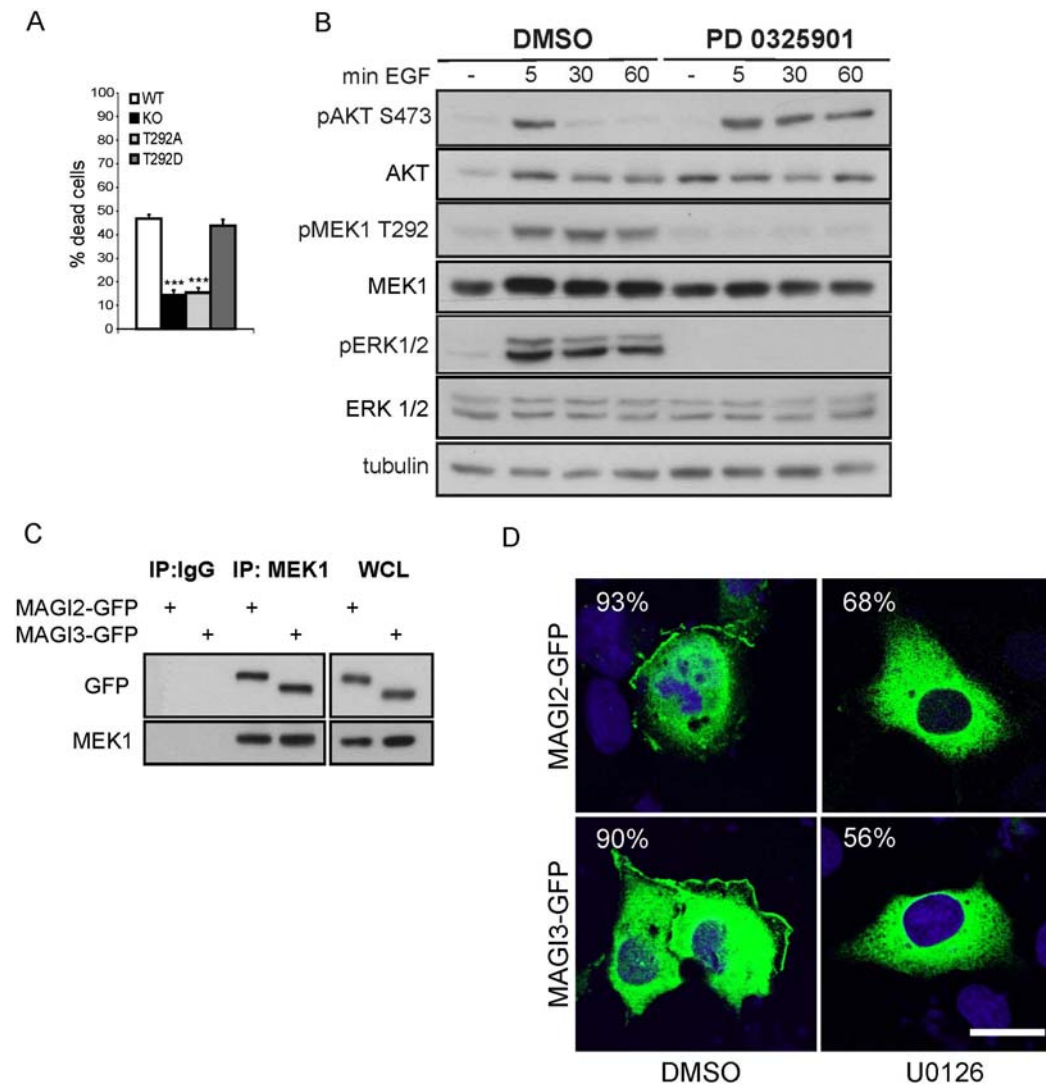


**Figure S5. T292 phosphorylation, but not MEK1 kinase activity, promotes MEK1/MAGI1/PTEN binding and decreases PIP<sub>3</sub> pathway activation, Related to Figure 6**

**A**, WT, KO and MEK1 mutants expressing MEFs were treated with TNF $\alpha$  (10ng/ml)/cycloheximide (5 $\mu$ g/ml) for 16 hours. Cell death was analyzed by propidium iodide staining. The graph shows mean of three experiments  $\pm$  SD (error bars). \* < 0.05; \*\* < 0.01; \*\*\* < 0.001. **B**, WT MEFs were pretreated with PD0325901 or DMSO (vehicle) and stimulated with EGF for the indicated times. Whole cell lysates were subjected to immunoblot analysis with the indicated antibodies. Tubulin is shown as a loading control. **C-D**, MAGI2 and 3 interact with MEK1 and their membrane localization is affected by chemical inhibition of MEK1 T292 phosphorylation. COS7 cells were transfected with MAGI2-GFP and MAGI-3-GFP plasmids. Immunoprecipitation was performed using a MEK1 or an irrelevant (IgG) antibody. In **D**, membrane of MAGI2 and 3 was determined in cells treated with the MEK1 inhibitor U0126 or with the vehicle DMSO. The percentage of cells showing MAGI2 or MAGI3 membrane localization is shown in the insets.

## Supplemental Experimental Procedures

### Immunofluorescence

Methanol-fixed MEFs were stained with anti-PTEN (Santa Cruz) and goat anti-mouse Alexa488 secondary antibody (Invitrogen). MEFs were fixed in 4% PFA, permeabilized with saponin and stained with anti-PIP<sub>3</sub>-FITC antibody (Echelon) was used. Slides were mounted with Vectashield with DAPI (Vector Laboratories). The frequency of membrane recruitment was established by counting cells in five to ten microscopic fields per experimental condition (300 cells) in at least three independent experiments. Images were acquired with Upright point scanning confocal microscope Zeiss LSM-510 Meta. Following lasers were used: Laser Diode 405nm; 25mW (violet) and Argon 458, 477, 488, 514nm; 30mW (blue). Images were taken with 63x/1.40 plan-apochromat Oil, DIC III objective and Zeiss ZEN 2009, v 5.5.0.443 software running on Windows7-64-bit PC.

### Colony forming assays

Colony forming assays were performed as described (Miller et al., 2008). Briefly, total bone marrow cells or total splenocytes were seeded in semisolid media (StemCell Technologies) containing 10 ng/ml rmIL-3, 50 ng/ml rmSCF (both from StemCell Technologies) and 10 ng/ml rhIL-6 (eBioscience) for determination of CFU-C or in media containing 3U/ml EPO for counting CFU-E and BFU. We counted myeloid colonies (CFU-GM, CFU-M and CFU-G) and immature BFU-E on day 7; mature CFU-E were counted on day 2.

### Lymphocyte proliferation and activation

Expression of CD69 was assessed after 4 days of stimulation with  $\alpha$ -IgM (5  $\mu$ g/ml, Jackson ImmunoResearch) and BAFF (10 ng/ml, R&D) in the case of B cells and 1  $\mu$ g/ml CD3 and CD28 in the case of CD4<sup>+</sup> T cells. Proliferation of B and CD4<sup>+</sup> T lymphocytes was analyzed by staining with Cell Trace Violet (Invitrogen) after 4 days of activation with the same stimuli.

### Cytokine flow cytometry

Total splenocytes were stimulated with Cell Stimulation Cocktail with protein transport inhibitors (eBioscience) and LPS (5 ng/ml, Sigma) for 6 hours. Cells were then stained with anti-CD4, fixed, permeabilized (BD Cytofix/Cytoperm kit) and stained with following antibodies: GM-CSF, IL-10 (eBioscience), TGF $\beta$  (LifeSpan Biosciences) and IFN $\gamma$  (BD). BAFF expression on the surface of freshly isolated splenocytes was detected by BAFF antibody (LifeSpan Biosciences).

### Plasmids

MAGI2-GFP and MAGI3-GFP plasmids were provided from Zhigang Xu. MAGI1 deletion mutants were obtained by site-directed mutagenesis of full length myc-MAGI1 (Chiu et al., 2004) using the following primers:

$\Delta$ GUK: 5'-CTACCTCTTCTGCAGAG-3', 5'-AAGGGGTCTCCAGATCATCTACCTCTTCTGCAGAG-3'  
5'-CTGGAACCGTTGGTTGAG-3', 5'-ATGATCTGGAGACCCCTTCTGGAACCGTTGGTTGAG-3'  
 $\Delta$  WW: 5'-CTAGAAGCCAAACGGAAG-3', 5'-CCTGAAAAGTGGGAGATGCTAGAAGCCAAACGGAAG-3',  
5'-TAGAGGACCTAAATTATC-3', 5'-CATCTCCAGTTTTAGGTAGAGGACCTAAATTATC-3'  
 $\Delta$ GUK-WW: 5'-CTAGAAGCCAAACGGAAG-3',  
5'-AAGGGGTCTCCAGATCATCTAGAAGCCAAACGGAAG-3', 5'-CTGGAACCGTTGGTTGAG-3',  
5'-ATGATCTGGAGACCCCTTCTGGAACCGTTGGTTGAG-3'

The myc-GUK-WW construct was generated by amplifying the relevant fragment of the full length MAGI1 plasmid using the following primers:

5'-CTAGCTAGCATGGCATCAATGCAGAAGCTGATCTCAGAGGAGGACCTGAGGCTCAACAAGGACCTACG-3' and 5'-CGCGGATCCTTAATGGGAAGGAGCAACAGGAG-3' followed by recloning into pcDNA3.1 plasmid.

QuikChange Site-Directed Mutagenesis Kit (Stratagene) was used to introduce point mutations in WW domains. All constructs were verified by sequencing to harbor the correct mutation.

WW1 mutation Y to A: 5'-CCTATACTGAAAATGGAGAAGTCGCTTTCATAGACCACAACACG-3' and 5'-CGTGTGTGGTCTATGAAAGCGACTTCTCCATTTTCAGTATAGG-3'

WW2 mutation Y to A: 5'-CCCTGTCTACGGTGTGCGCTATGTAGACCACATCAACAGG-3' and 5'-CCTGTTGATGTGGTCTACATAGGCGACACCGTAGACAGGG-3'

### **Antibodies**

For immunoprecipitation: MEK1, MEK2; BD Transduction Labs; myc tag, E. Ogris, MFPL, Vienna; PTEN, Santa Cruz; all 1:100.

For immunoblotting: AKT, pAKT S473, pAKT T308, p85, p110 $\alpha$ , MEK1, pMEK S218/222, pMEK1 S298, PTEN, pPTEN 380/382/383, npPTEN 380/382/383, pERK, ERK, pmTOR S2448, mTOR, pGSK3 $\beta$  S9, pS6K T389, IGF1R, GAPDH, myc tag (Cell Signaling), MAGI-1, actin, FAK (Santa Cruz), pFAKY397, caveolin, MEK2 (BD Transduction Laboratories), tubulin (Sigma), pMEK1 T292 (Upstate), his tag (Rockland), MAGI2 (Millipore), MAGI3 (Abcam).

### **Supplemental References**

Chiu, J., March, P.E., Lee, R., and Tillett, D. (2004). Site-directed, Ligase-Independent Mutagenesis (SLIM): a single-tube methodology approaching 100% efficiency in 4 h. *Nucleic Acids Research* 32, e174.

Miller, C.L., Dykstra, B., and Eaves, C.J. (2008). Characterization of mouse hematopoietic stem and progenitor cells. *Current protocols in immunology* / edited by John E Coligan [et al] *Chapter 22, Unit 22B 22*.